

Analysis of Inductance in Workpiece according to High-Frequency of Induction Heater for Electric Vehicle

Hui-Seong Shin¹, Chung-Hui Lee², Ki-Chan Kim*³

¹ Mater course, Department of Electrical Engineering, Hanbat National University, Daejeon, 34158 Korea

² Mater course, Department of Electrical Engineering, Hanbat National University, Daejeon, 34158 Korea

*³ Professor, Department of Electrical Engineering, Hanbat National University, Daejeon, 34158 Korea

Abstract.

BACKGROUND/OBJECTIVES: Induction heater for electric vehicle have skin effect due to the influence of high frequency. And the influence of the skin effect, which is an AC loss, must be reduced.

METHODS/STATISTICAL ANALYSIS: Reducing the skin effect is to alleviate the magnetic saturation of the workpiece surface. When magnetic saturation occurs, the magneto-resistance rapidly increases, so a design capable of mitigating the magneto-resistance is required. FEM analysis was performed to analyze the skin effect. If the magneto-resistance increases, the amount of magnetic flux leaked will increase, and the amount of leakage is checked by deriving inductance.

FINDINGS: Magnetic saturation is related to magnetic reluctance. Magnetic reluctance is inverse proportion to the cross-sectional area of the workpiece through which the magnet passes. And magnetic reluctance has an inverse proportion relationship with inductance. When the cross-sectional area of the work piece was increased to reduce the skin effect, the total inductance increased, but the amount of leaked inductance also increased. The increase in leakage inductance acts as a loss, not heat generation of the work piece, and means an increase in the amount of leakage of magnetic flux in the work piece of the induction heater. The amount of leakage inductance increased to reduce the skin effect, and when the amount of leakage inductance was reduced, the skin effect increased. In this paper, about 11kW class induction heater was analyzed and the increase in leakage inductance was analyzed for the total inductance according to the surface of the workpiece. In addition, the trade-off between skin effect and leakage inductance was analyzed.

IMPROVEMENTS/APPLICATIONS: The optimal design considering leakage inductance and skin effect reduces the volume of induction heater and can be applied to shielding design of induction heater.

Keywords: *Electric vehicle, Induction heater, High frequency, Skin effect, Magnetic reluctance, leakage inductance*

1. INTRODUCTION

If the battery does not maintain proper temperature conditions, its efficiency will decrease. Induction heater can be used to keep the battery of electric vehicle at an appropriate temperature. Induction heater can raise the desired temperature from low temperatures in a very short time. However, induction heaters operate at high frequency and the skin effect occurs at high frequencies. The skin effect is a phenomenon in which high-frequency current creates a magnetic field that interferes with the current flow inside the wire, and the current does not flow to the center of the wire[1][2]. This skin effect causes the magnetic skin effect and increases the magnetic reluctance of the workpiece surface. Magnetic reluctance increases due to the magnetic skin effect. And magnetic reluctance interferes with the flow of magnetic flux. Reducing the magnetic reluctance may increase the magnetic flux connected to the inside of the work piece and reduce the magnetic skin effect[3][4]. The induction heater uses high-frequency current to link the generated magnetic flux to the work piece. At this time, it is used as heat by using the iron loss generated in the work piece by the high frequency magnetic flux. Induction heater, when a current flow through a terminal connected to an AC power source, a magnetic flux that changes in size and direction over time is generated around the coil[5]. The generated magnetic flux causes iron loss in the conductor. Since the magnetic flux generated at this time alternates at a high frequency, the leakage magnetic flux increases due to the skin effect on the workpiece. In addition, since the distance to the work piece is not close when viewed from the side of the magnetic flux generated by the induction heater, the amount of magnetic flux leaked increases. Therefore, the size of the leakage inductance increases. Design in the direction of decreasing the leakage inductance through proper design is required[6].

2. SIMULATION MODEL AND CONDITION

2.1. SIMULATION MODEL

2.1.1. DESIGN FLOWCHART

The simulated induction heater consists of a coil that receives an AC voltage and generates a magnetic flux. The magnetic flux created by the AC voltage is connected to the workpiece, resulting in iron loss. Figure 1 is a flow diagram of the base model design for an induction heater simulation. First, to meet the capacity of the induction heater selected as 11kW, the applied voltage was determined to be 360Vdc. As for frequency, capacitance was determined under the condition of generating LC resonance at 30kW, and resistance was selected according to the flow chart. Designed with 2D and 3D models. However, considering that it takes a little longer for 3D analysis, it was analyzed in 2D. Next, I selected a resistor and performed a simulation. If the simulation results were not suitable, feedback was performed, and the final model was derived.

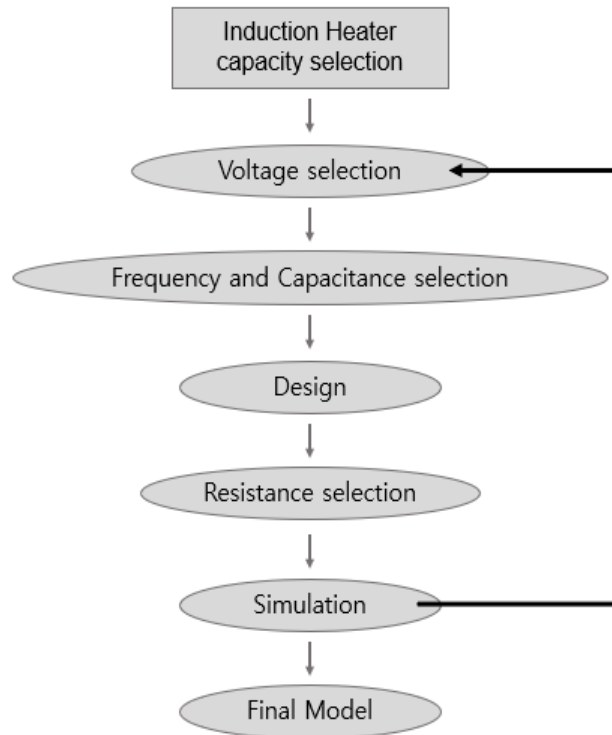


Figure 1. Induction Heater base model design flowchart

The specifications of the induction heater selected as the base model are shown in Table 1. The diameter of the workpiece is proportional to the capacity of the induction heater, and the inner diameter is 15mm and the outer diameter is 26.4mm. To distinguish the size of the inductance according to the surface width of the workpiece, the inner and outer surface widths of the workpiece were selected equally. As mentioned above, the capacity and frequency were selected as 11kW and 30kHz. FEM was conducted by voltage source analysis. And it was derived that 33A flows through the coil composed of 51 turns.

Table 1. Specification of induction heater selected as base model

Parameter	Value	Unit
Inner diameter of workpiece	15	mm
Outer diameter of workpiece	26.4	mm
Inner surface width of workpiece	1.36	mm
Outer surface width of workpiece	1.36	mm
Capacity	11	kW
Frequency	30	kHz
Voltage	360	Vdc
Current	33	A
Number of turns of the coil	51	-

2.2. CONDITION

2.2.1. LC RESONANCE CIRCUIT

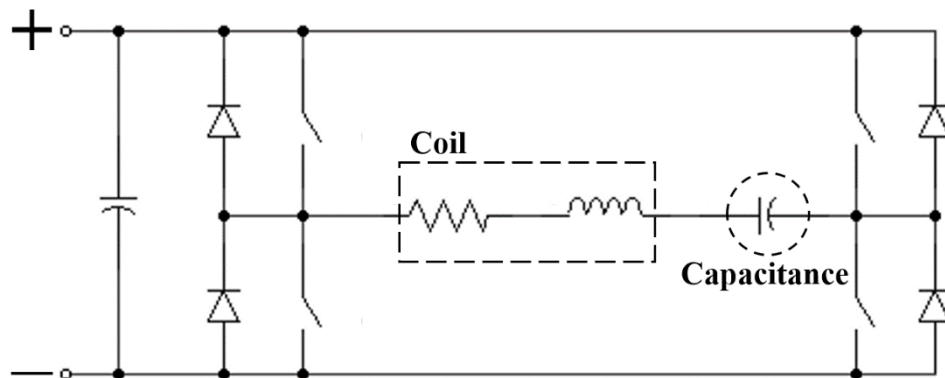


Figure 2. LC resonance circuit used for cosimulation

Resonant frequency means that the natural frequency determined by the inductance and capacitance contained in the circuit matches the frequency of the power supply. The resonance circuit is divided into series resonance and parallel resonance. The induction heater model used in this study was composed of a control circuit using a series resonance circuit. When the resonant frequency operation is performed in the series resonant circuit, the reactance component is lowered, and the operation of a high-power factor becomes possible. In a series resonant circuit, the largest current can flow through the circuit if the condition of the resonant frequency is met.[7-9]

$$L = \frac{e}{2\pi f I} \quad (1)$$

$$f_0 = \frac{1}{2\pi\sqrt{LC}} \quad (2)$$

Equation (1) is used to derive the inductance of the entire induction heater. After applying a frequency of 30 kHz to derive the induced electromotive force and current, the inductance of the entire induction heater can be derived. Equation (2) is used to derive the resonant frequency. The LC resonance circuit for coupled analysis is completed by deriving the inductance of the entire induction heater through Equation (1) and applying it to the capacitance shown in the circuit in Figure 2 so that LC resonance occurs at 30kHz.[10]

2.2.2. BASE MODEL DESIGN

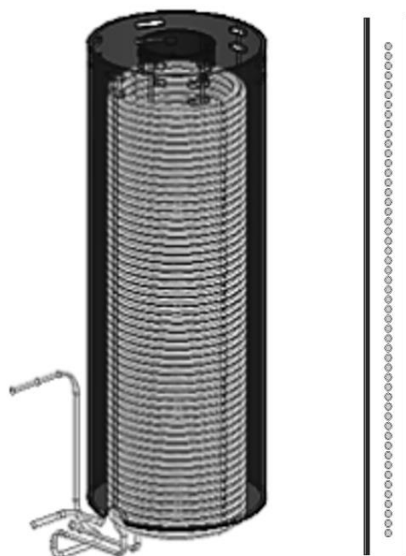


Figure 3. 3D & 2D induction heater model designed for FEM analysis

Figure 3 is an induction heater base model that will coupled analysis the LC resonance circuit shown in Figure 2. Both 3D and 2D were designed, and 2D models were used for FEM analysis to shorten the time. In addition, since the flux linkage is concentrated on the surface of the work piece due to the skin effect, the work piece is divided more densely as it gets closer to the coil.

3. FEM SIMULATION

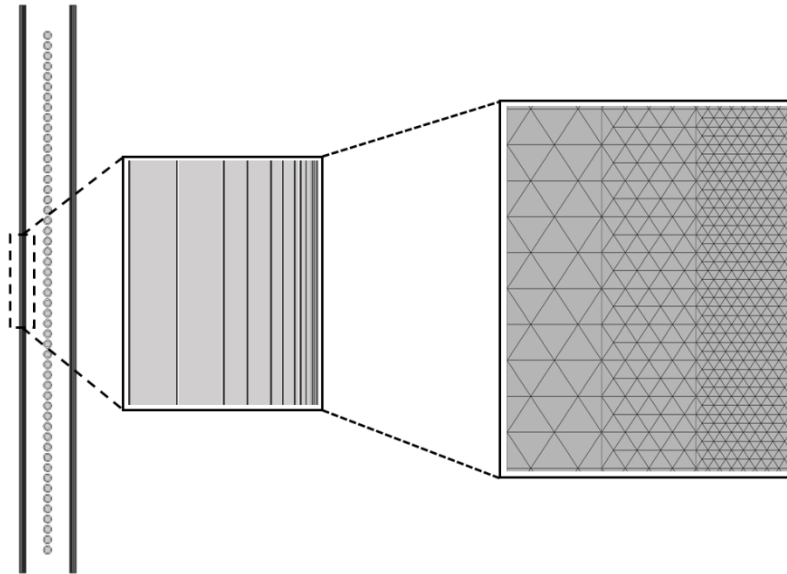


Figure 4. The divided workpiece and the mesh of the workpiece

Figure 4 shows the subdivision of the base model workpiece. It also shows the mesh divided into three areas. In the area adjacent to the coil, the change in magnetic flux is large, so the mesh must be set densely. To find out the scale of the skin effect, the current density vector of the workpiece was derived. Figure 5 is the result of the derived current density vector of the workpiece. As expected, the current density vector of the workpiece was concentrated on the surface of the workpiece, and it was found that the current density vector of the internal workpiece was larger than that of the external workpiece [11-14].

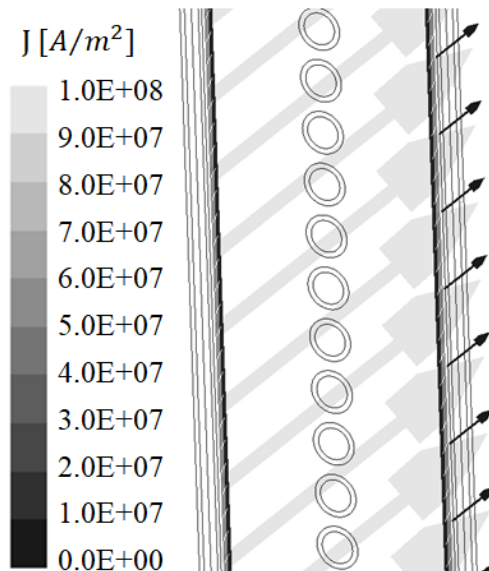


Figure 5. Current density vector of workpiece

When the current density vector was confirmed compared to the magnetic flux diagram, the effect of the skin effect could be clearly expressed. By dividing the surface width of the workpiece step by step, the total inductance of the induction heater and the inductance of the workpiece were derived. The surface width of the workpiece was divided into 5 steps [15][16].

Table 2. Derivation of leakage inductance according to the surface width of the workpiece

Surface width of the workpiece	Inductance of the entire induction heater [μH]	Induction of workpiece [μH]	Leakage inductance [μH]	Leakage inductance per total inductance [%]
0.64	92.53	77.93	17.60	19.02
1.00	89.70	62.72	26.98	30.08
1.36	86.87	57.77	29.1	33.50
1.72	78.27	55.76	22.51	28.76
2.08	66.60	48.95	17.65	26.50

$$\delta = \frac{1}{\sqrt{\pi f \mu \sigma}} \quad (3)$$

Table 2 is the result of FEM analysis by dividing the workpiece surface width into 5 steps. The analysis was conducted by

dividing the surface width of the workpiece including the base model into 5 steps of 0.36mm each. As the surface width of the workpiece becomes thicker, the magnetoresistance decreases, so the inductance must increase. As a result, the inductance increases as the width of the workpiece surface increases up to the penetration depth region expressed in Equation (3). However, as the surface width of the workpiece increases, the area in which magnetic flux other than the penetration depth cannot be interlinked increases, so the inductance decreases for the entire area. When the inductance was checked over the entire area of the workpiece, the inductance of the workpiece decreased as the surface width increased, and the leakage inductance was the lowest as the surface width of the workpiece narrowed.

4. CONCLUSION

This paper analyzes the inductance of the work piece that affects the efficiency of the induction heater. The leakage inductance was derived through FEM analysis, and the relationship of the leakage inductance according to the surface width of the workpiece was analyzed. Through this study, it was confirmed that an appropriate design is required between the reduction of the skin effect and the reduction of the leakage component. As a result, it is possible to apply a design that increases the efficiency by reducing the skin effect and leakage components of the induction heater.

5. ACKNOWLEDGMENT

This work was supported by the National Research Foundation of Korea(NRF) grant funded by the Korea government(MSIT) (No. NRF-2019R1F1A1058504)

6. REFERENCES

1. A. Boadi, Y. Tsuchida, T. Todaka and M. Enokizono. Designing of suitable construction of high-frequency induction heating coil by using finite-element method. *IEEE Transactions on Magnetics*. Oct. 2005; vol. 41, no. 10, pp. 4048-4050. DOI: 10.1109/TMAG.2005.854993.
2. M. Messadi et al. Eddy Current Computation in Translational Motion Conductive Plate of an Induction Heater with Consideration of Finite Length Extremity Effects. *IEEE Transactions on Magnetics*. March 2016; vol. 52, no. 3, pp. 1-4. DOI: 10.1109/TMAG.2015.2498762.
3. M. Enokizono and H. Tanabe. Numerical analysis of high-frequency induction heating including temperature dependence of material characteristics. *IEEE Transactions on Magnetics*. July 1995; vol. 31, no. 4, pp. 2438-2444. DOI: 10.1109/20.390154.
4. J. Acero, R. Alonso, J. M. Burdío, L. A. Barragan and D. Puyal. Frequency-dependent resistance in Litz-wire planar windings for domestic induction heating appliances. *IEEE Transactions on Power Electronics*. July 2006; vol. 21, no. 4, pp. 856-866. DOI: 10.1109/TPEL.2006.876894.
5. J. Lee, S. Lim, K. Nam and D. Choi. An Optimal Selection of Induction-Heater Capacitance Considering Dissipation Loss Caused by ESR. July-aug. 2007; vol. 43, no. 4, pp. 1117-1125. DOI: 10.1109/TIA.2007.900490.
6. M. Runde and N. Magnusson. Design, building and testing of a 10 kW superconducting induction heater. June 2003; vol. 13, no. 2, pp. 1612-1615. DOI: 10.1109/TASC.2003.812806.
7. Ó. Lucía, J. M. Burdío, L. A. Barragán, J. Acero and I. Millán. Series-Resonant Multiinverter for Multiple Induction Heaters. *IEEE Transactions on Power Electronics*. Nov. 2010; vol. 25, no. 11, pp. 2860-2868. DOI: 10.1109/TPEL.2010.2051041.
8. Hyun-Seob Cho. Design of Noise Reduction Output Filter for Induction Motor Using H-Bridge Inverter. *Journal of Next-generation Convergence Technology Association*. 2020 December; 4(6):595-600.
9. D. Kim, J. So and D. Kim. Study on Heating Performance Improvement of Practical Induction Heating Rice Cooker With Magnetic Flux Concentrator. *IEEE Transactions on Applied Superconductivity*. June 2016; vol. 26, no. 4, pp. 1-4. DOI: 10.1109/TASC.2016.2540650.
10. W. Han, K. T. Chau and Z. Zhang. Flexible Induction Heating Using Magnetic Resonant Coupling. *IEEE Transactions on Industrial Electronics*. March 2017; vol. 64, no. 3, pp. 1982-1992. DOI: 10.1109/TIE.2016.2620099.
11. Young-Sun Kim. Application of LSM in Optimization Technique of Electric and Magnetic Field System. *Journal of Next-generation Convergence Technology Association*. 2020 December; 4(6):601-608.
12. H. Kurose, D. Miyagi, N. Takahashi, N. Uchida and K. Kawanaka. 3-D Eddy Current Analysis of Induction Heating Apparatus Considering Heat Emission, Heat Conduction, and Temperature Dependence of Magnetic Characteristics. *IEEE Transactions on Magnetics*. March 2009; vol. 45, no. 3, pp. 1847-1850. DOI: 10.1109/TMAG.2009.2012829.
13. M. Enokizono, T. Todaka and S. Nishimura. Finite element analysis of high-frequency induction heating problems considering inhomogeneous flow of exciting currents. *IEEE Transactions on Magnetics*. May 1999; vol. 35, no. 3, pp. 1646-1649, DOI: 10.1109/20.767321.
14. Yong-Min You. Shape Optimization of PMSM Based on Automated Design of Experiments and Multi-layer Perceptron. *Journal of Next-generation Convergence Technology Association*. 2020 October; 4(5):478-484.
15. Y. Wang et al. Study on No-Insulation HTS Pancake Coils With Iron Core for Superconducting DC Induction Heaters. *IEEE Transactions on Applied Superconductivity*. June 2015; vol. 25, no. 3, pp. 1-5. DOI: 10.1109/TASC.2014.2361932.
16. J. Ma et al. Experimental and Numerical Study of a DC Induction Heater Prototype With an Adjustable Air Gap Structure. *IEEE Transactions on Applied Superconductivity*. June 2016; vol. 26, no. 4, pp. 1-5. DOI: 10.1109/TASC.2016.2515081.